Journal of Applied Polymer Science

Transparency of Rubber-Toughened Polymer Blend Containing Plasticizer

Shuji Takahashi,[1,2] Shogo Nobukawa,[1] Masayuki Yamaguchi[1]

[1]School of Materials Science, Japan Advanced Institute of Science and Technology, Nomi, Ishikawa 923-1292, Japan

[2]Vehicle Line I, Suzuki Motor Corporation, Hamamatsu, Shizuoka 432-8611, Japan

Correspondence to: M. Yamaguchi (E-mail: m_yama@jaist.ac.jp)

ABSTRACT: Transparency and its temperature dependence were studied for rubber-toughened polymer blends composed of poly(methyl methacrylate), core–shell latex–rubber particles, and plasticizers such as tricresyl phosphate and di(2-ethylhexyl)adipate. The transparency of the blends was found to be improved by the addition of the plasticizers. This phenomenon is attributed to the uneven distribution of the plasticizer in the blends. Furthermore, it was found that the plasticizers improve the transparency in a wide temperature range, because the plasticizer addition reduces the difference in the thermal expansion, and thus the temperature dependence of the refractive index, between poly(methyl methacrylate) and the rubber phases. © 2014 Wiley Periodicals, Inc. J. Appl. Polym. Sci. **2014**, *131*, 40775.

KEYWORDS: blends; optical properties; plasticizer; structure-property relations

Received 4 January 2014; accepted 27 March 2014

DOI: 10.1002/app.40775

INTRODUCTION

Because most decorating plastics in an automobile interior are painted, intense attention has been focused on the reduction of volatile organic compounds. In particular, the demand for paintless products is rapidly increasing these days to reduce the risk of our health and environmental problems. In the field of automobile parts, transparent glassy polymers are greatly investigated to be used instead of painted products, because they can provide good quality of colors by the addition of various pigments. One of the most famous candidates among transparent polymers is poly(methyl methacrylate) (PMMA) because of its remarkable optical transparency and good weatherability. However, the improvement of mechanical toughness of PMMA is inevitable to widen the applications especially for automobile interior.

After commercialization of high-impact polystyrene, the rubber-blend technology was studied to improve the toughness of plastics.[1] However, it is significantly difficult for rubber-toughened polymer blends to reduce light scattering owing to the difference in the refractive index between the two phases. In general, both minimizing the refractive index difference and reducing the size of dispersed particles are required to provide transparency.[2–8] Recently, specific core–shell latex–rubber particles (CSL) have been developed and are commercially available as an impact modifier of PMMA without losing the transparency. The inner core of CSL consists of a cross-linked copolymer of acrylic esters, which act as a rubber having the same refractive index with PMMA.[9] On the other hand, the outer shell is composed of PMMA to show good dispersion in the matrix, i.e., PMMA.[10] The size of CSL can be controlled by the surfactant concentration at the emulsion polymerization.[11]

Up to now, several studies have been carried out on PMMA/CSL blends to clarify the effect of characteristics of CSL on the impact strength, such as chemical structure of the core,[12] core/shell volume ratio,[13] particle size,[14,15] and the number of layers.[16,17] Wrotecki et al.[14] reported that the optimal size for CSL to improve the toughness of PMMA is 200–250 nm. Lovell et al.[16] studied the toughening behavior of multilayered particles and demonstrated that the particles with three and four layers were more effective to enhance the toughness of PMMA. Finally, a new concept has been proposed for the CSL blend technology recently, in which a rigid plastic is in the core surrounded by a rubbery soft material as the shell.[18–22] The introduction of a rigid core prohibits the transversal contraction after void opening at the poles of CSL under stress field, and thus provides a large volume strain due to stabilization of cavitation. Consequently, marked energy dissipation is achieved by shear yielding in the matrix polymeric ligand.

As compared with various efforts to improve the mechanical toughness, however, few studies have been reported on the transparency of PMMA/CSL blends. Park et al.[23] investigated both mechanical and optical properties of rubber-toughened PMMA containing poly(urethane acrylate)/PMMA core–shell particles. They successfully improved the toughness without losing

Table I. Characteristics of Samples

Sample code	Density (kg/m^3)[a]	Refractive index[b]
PMMA	1190	1.490
CSL	1170	1.496
TCP	1170	1.557
DOA	927	1.445

[a] Reference values of supplier.
[b] Measured values by Abbe refract meter.

transparency by adjusting the refractive index of poly(urethane acrylate), i.e., the core phase. Furthermore, Song et al.[24] obtained a transparent blend with rubbery poly(butylacrylate-*co*-styrene) cross-linked by divinylbenzene having a high refractive index. According to them, the refractive index of the rubber cross-linked by 1 wt % of divinylbenzene is almost identical to that of PMMA.

The transparency of rubber-toughened polymer blends, in general, depends on the ambient temperature. This phenomenon is attributed to the difference in the temperature dependence of the refractive index, because the thermal expansion coefficient of a rubbery material is usually larger than that of a glassy polymer.[25–28]

In this study, the effect of a plasticizer on the optical transparency for the blends of PMMA and CSL was investigated. In particular, the transparency in the wide temperature range was studied with the evaluation of the thermal expansion. The plasticizers used were tricresyl phosphate (TCP) and di(2-ethylhexyl)adipate (DOA). The former has a higher refractive index and the latter has a lower one than the polymeric materials, i.e., PMMA and CSL.

EXPERIMENTAL

Materials

A commercially available PMMA (Sumipex LG-21; Sumitomo Chemical, Japan) was used in this study. The number-average molecular weight and polydispersity of PMMA, evaluated by size-exclusion chromatography, are as follows: $M_n = 4.4 \times 10^4$ and $M_w/M_n = 1.89$.

CSL (Staphyloid IM-701; Ganz Chemical, Japan), produced by seed emulsion polymerization, were also used. The content of PMMA as the shell is 30 wt %. The rubbery core is composed of cross-linked poly(styrene-*co*-ethylacrylate). The diameter of particles is approximately 170 nm, which was measured by the light scattering method.

Plasticizers used in this study were TCP and DOA. Both of them were produced by Daihachi Chemical Industry, Japan. The characteristics of TCP and DOA are summarized in Table I with those of PMMA and CSL. The refractive indices at room temperature are 1.557 (TCP) and 1.445 (DOA).

Sample Preparation

PMMA and CSL were mechanically blended with one of the plasticizers in the molten state. The blend ratios of PMMA/CSL/plasticizer were 80/20/0, 5, 10, 15, and 20 in the weight fraction. Although CSL used in this study is known to show a good thermal stability, thermal stabilizers such as hindered phenol (Irganox 1010; Ciba, Switzerland) and phosphate (Irgafos 168; Ciba) were further added to prevent the thermal degradation of the CSL core. The amount of each thermal stabilizer was 0.5 wt %.

Compounding was performed by a counter-rotating twin-screw extruder (KTX-30; Kobe Steel, Japan) at a screw rotation speed of 200 rpm. The temperature of the barrel and die was controlled at 200°C. Prior to melt-mixing, the polymers were dried under vacuum at 60°C for 3 h. Furthermore, PMMA/plasticizer and CSL/plasticizer with various blend ratios were also prepared by the same method. In this study, the numerals in the sample code represent "phr" (parts per hundred parts by weight of a resin) of the plasticizers. For example, PMMA/CSL/TCP20 is the blend containing 20 phr of TCP, i.e., PMMA/CSL/TCP = 80/20/20.

The pellets obtained were compressed into flat sheets with 2.0 mm thickness by a laboratory compression-molding machine at 200°C under 10 MPa for 10 min. Then, the sample was subsequently cooled at 20°C for 5 min.

Measurements

Refractive index was measured at 20°C by an Abbe refractometer (NAR-1T; Atago, Japan), with methylene iodide as the contact liquid. The wavelength measured was 589 nm. The transparency of the sheet samples was evaluated by a haze meter (HZ-2; Suga Test Instruments, Japan). The haze value is defined as the percentage of total transmitted light passing through a specimen that is scattered from the incident beam from 2.5° to 90°.

$$\text{Haze}\ (\%) = T_d/T_t \times 100 \quad (1)$$

where T_d and T_t are the intensities of transmitted diffused light and total transmitted light, respectively. Therefore, a transparent material shows a low value of haze.

In addition, to evaluate the temperature dependence of the transparency, light transmittance was measured at various temperatures using an ultraviolet-visible spectrometer (Lamba25; PerkinElmer, Waltham, MA) equipped with a temperature controller. The light transmittance T is determined by the following relation:

$$T(\%) = T_1/T_0 \times 100 \quad (2)$$

where T_1 is the intensity of the transmittance light; i.e., $T_t - T_d$, and T_0 is that of the incident light.

The morphology of the blends was examined by a field-emission scanning electron microscope (JSM-7001F; JEOL, Japan). Prior to the observation, the surface of the cryogenically fractured samples was coated by platinum–palladium.

The temperature dependence of oscillatory tensile modulus in the solid state, such as tensile storage modulus E' and loss modulus E'', was measured by a dynamic mechanical analyzer (E4000; UBM, Japan) in the temperature range between −80°C and 150°C. The heating rate was 2°C/min, and the applied frequency was 10 Hz. The rectangular samples with the dimension

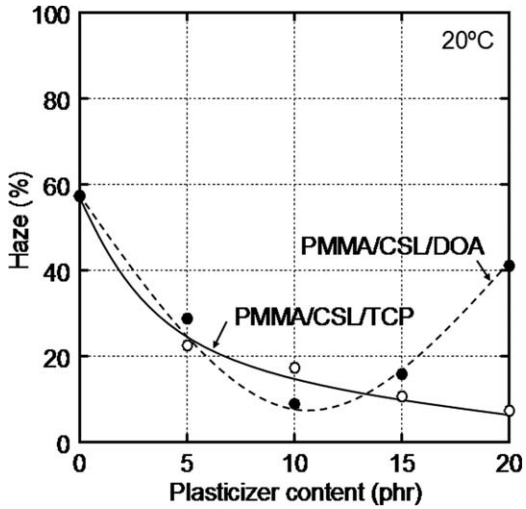

Figure 1. Haze values at 20°C for PMMA/CSL (80/20) blends containing various amounts of TCP (open circles) and DOA (closed circles).

of 4 mm × 25 mm × 2 mm were cut out from the compressed sheets.

The linear coefficient of thermal expansion was measured by a thermo-mechanical analyzer (TMA4000SA; Bruker, Billerica, MA) from 20°C to 80°C at a heating rate of 2°C/min. A constant load, 50 mN, was applied in a compression mode. The rectangular samples with the dimension of 5 mm × 5 mm × 2 mm were cut out from the sheets.

RESULTS AND DISCUSSION

Transparency at Room Temperature

Figure 1 shows the haze values at 20°C for the blends with various amounts of plasticizers. The thickness of the samples was 2.0 mm. The haze value is often used as a measure of the turbidity of films and sheets in industry. The value can be predicted based on the scattering theory as explained in detail by Willmouth.[5] Furthermore, Khanarian[7] successfully confirmed

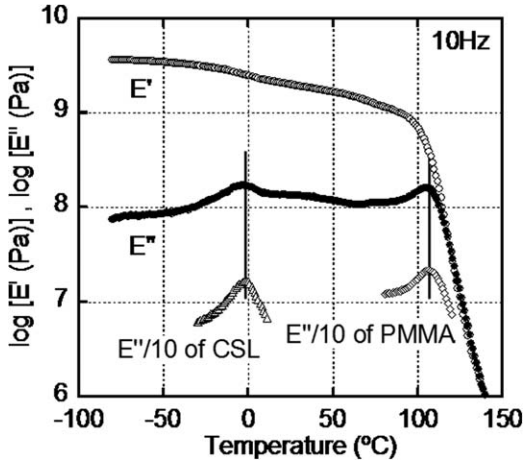

Figure 2. Temperature dependence of tensile storage modulus E' (open circles) and loss modulus E'' (closed circles) at 10 Hz for PMMA/CSL (80/20). In the figure, E'' curves around T_g for pure CSL (triangles) and pure PMMA (diamonds) are also shown with a vertical shift.

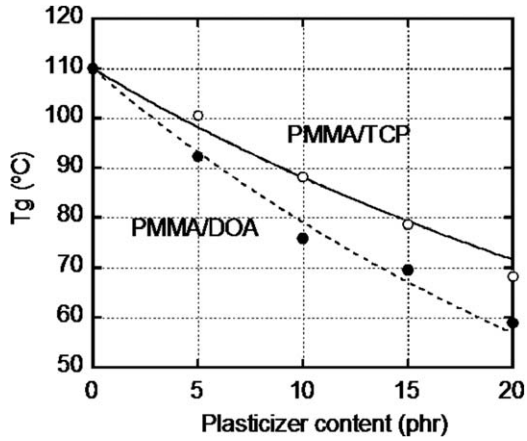

Figure 3. Effect of the plasticizer content on T_g for the binary blends PMMA/TCP (open circles) and PMMA/DOA (closed circles). The lines represent the values calculated from the Fox equation.

the agreement between the calculated values and the experimental results using immiscible polymer blends.

The binary blend without plasticizers, i.e., PMMA/CSL (80/20), shows a high value of haze, owing to light scattering originated from the difference in the refractive index; 1.490 for PMMA and 1.496 for CSL. The actual difference between the matrix PMMA and the rubbery core phase in CSL is larger, because the measured refractive index of CSL is the average value of the shell (PMMA) and core components. Considering the shell/core volume ratio, the refractive index of CSL core was calculated to be 1.4986, using the Gladstone–Dale relation [eq. (3)].[29,30]

$$n = \sum_i \phi_i n_i \tag{3}$$

where ϕ_i and n_i are the volume fraction and the refractive index of the i-component, respectively.

The figure demonstrates that the plasticizer addition affects the transparency of the blend. In particular, the blends containing a small amount, i.e., less than 10 phr, of the plasticizer show good transparency. This will be attributed to the decrease in the refractive index difference, as explained in detail later. In the

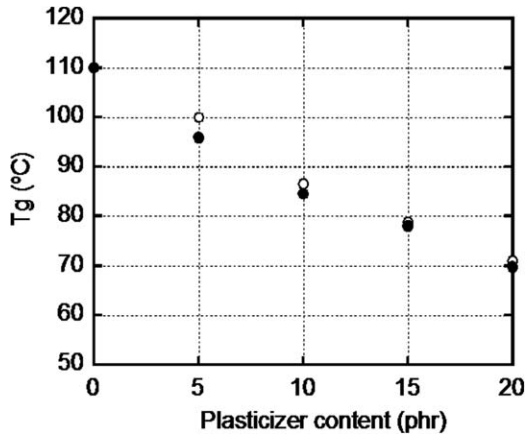

Figure 4. Effect of the plasticizer content on T_g of PMMA phase for the ternary blends PMMA/CSL/TCP (open circles) and PMMA/CSL/DOA (closed circles).

Table II. Plasticizer Content and Refractive Index of PMMA and CSL Core Phases

	PMMA phase		CSL core phase	
Sample Code	Plasticizer content[a]	Refractive index[b]	Plasticizer content[a]	Refractive index[b]
PMMA/CSL	0	1.4900	0	1.4986
PMMA/CSL/TCP5	4.52	1.4943	0.38	1.5011
PMMA/CSL/TCP10	9.29	1.4985	0.71	1.5028
PMMA/CSL/TCP15	13.88	1.5021	1.12	1.5048
PMMA/CSL/TCP20	18.49	1.5054	1.51	1.5066
PMMA/CSL/DOA5	4.12	1.4879	0.88	1.4958
PMMA/CSL/DOAIO	7.49	1.4864	2.51	1.4908
PMMA/CSL/DOA15	12.88	1.4845	3.12	1.4892
PMMA/CSL/DQA20	15.73	1.4843	4.27	1.4864

[a] Estimated by the peak temperature of E''
[b] Calculated by the Gladstone-Dale relation.

case of the TCP addition, the transparency monotonically increases in the experimental range even beyond 10 phr. In contrast, the haze value shows the minimum at 10 phr for the blends with DOA.

Dynamic Mechanical Properties

Figure 2 shows the temperature dependence of oscillatory tensile moduli such as storage modulus E' and loss modulus E'' in the solid state at 10 Hz for the binary PMMA/CSL blend. The storage modulus E' decreases slightly at around 0°C owing to the glass-to-rubber transition of the core component in the dispersed CSL. Then, E' drops off sharply around at 100°C, i.e., the glass-transition temperature T_g, of the matrix PMMA. Correspondingly, two peaks are detected in the E'' curve, demonstrating that the blend shows phase separation. Furthermore, the peaks of the blend appear at the same temperatures of individual pure components, as indicated in the figure.

Figure 3 shows the peak temperature of E'' ascribed to T_g for PMMA containing various amounts of the plasticizers. In the figure, the lines represent the values calculated using the Fox equation, $T_{g,\mathrm{blend}}$,

$$\frac{1}{T_{g,\mathrm{blend}}} = \frac{w_A}{T_{g,A}} + \frac{w_B}{T_{g,B}} \tag{4}$$

where $T_{g,i}$ and w_i are the glass-transition temperature and the weight fraction of the i-component, respectively.

As seen in the figure, T_g decreases with the plasticizer content in the experimental range, which corresponds with the predicted values. Moreover, the slope of the blends with DOA is found to be larger than that with TCP. It is reasonable because the solidification temperature of DOA (−65°C) is lower than that of TCP (−35°C). The plasticizer content in PMMA phase in the ternary blends can be easily predicted from the lines in the figure.

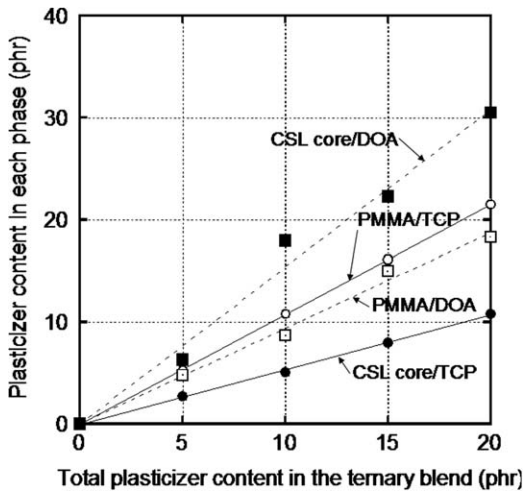

Figure 5. Relation between total amount of the plasticizer in the ternary blend and the plasticizer content in PMMA phase (open symbols) and CSL core phase (closed symbols), calculated from T_g: TCP (circles) and DOA (squares).

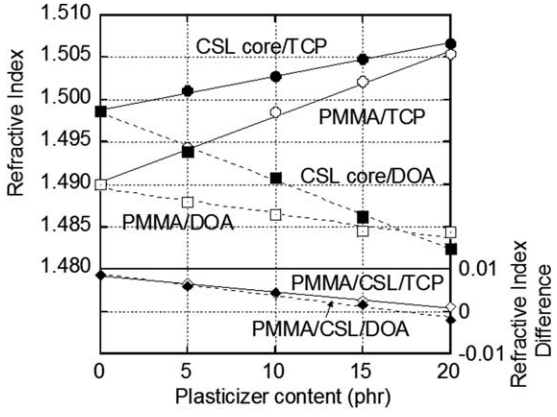

Figure 6. Relation between total amount of the plasticizer in the ternary blend and the refractive indices in PMMA phase (open symbols) and CSL core phase (closed symbols), calculated by the Gladstone–Dale relation: TCP (circles) and DOA (squares). The difference in the refractive index between PMMA and CSL core phases is also shown in the bottom of the figure: PMMA/CSL/TCP (open diamonds) and PMMA/CSL/DOA (closed diamonds).

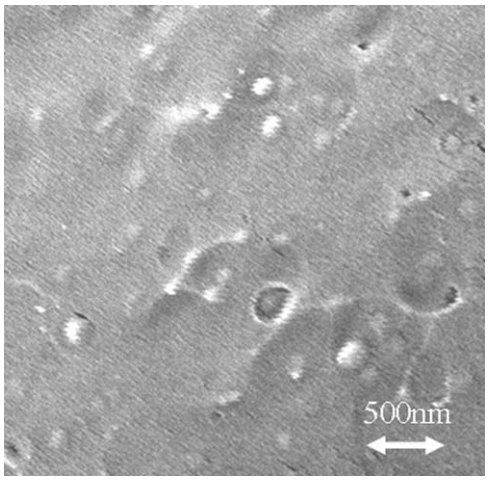

Figure 7. Field-emission scanning electron microscopy image of PMMA/CSL (80/20) blend.

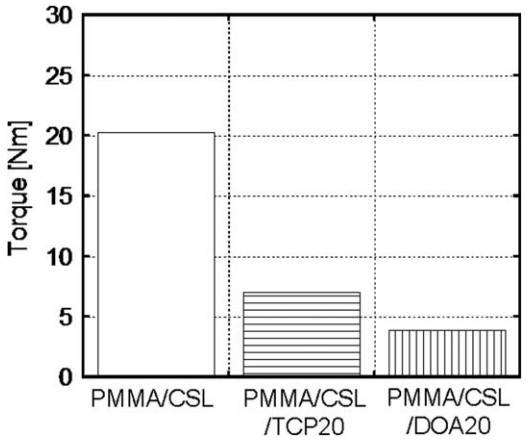

Figure 9. Mixing torque in the extruder for various samples.

Figure 4 shows T_g of PMMA phase in the ternary blends, i.e., PMMA/CSL/plasticizer. As similar to the previous figure, T_g of PMMA phase monotonically decreases with the plasticizer content. The slopes of the ternary blends are almost the same, irrespective of the species of the plasticizers, which is different from the result obtained for the binary blends, i.e., PMMA/plasticizer and CSL/plasticizer. This phenomenon suggests that more TCP resides in the PMMA phase for the ternary blends. The Hansen solubility parameters of PMMA, TCP, and DOA are 18.6, 19.0, and 17.6 $MPa^{1/2}$, respectively, indicating that PMMA prefers TCP to DOA.[31] Furthermore, the solubility parameter of the major component of CSL core, i.e., poly(ethylacrylate) is 17.6 $MPa^{1/2}$. Therefore, it is favorable for DOA to reside in the CSL core. In other words, uneven distribution of the plasticizers occurs in the ternary blends.

The plasticizer contents in PMMA phase, estimated from the dynamic mechanical spectra, are listed in Table II. Because the total amount of the plasticizer is known, the plasticizer content in CSL core can be also calculated. Using the plasticizer content in each phase, the refractive indices of PMMA and CSL core phases are predicted by eq. (3).

In Figure 5, the calculated plasticizer contents in both phases, as shown in Table II, are plotted against the total amount of the plasticizer in the ternary blends. It is confirmed from the figure that DOA tends to reside in the CSL core phase, whereas more TCP exists in PMMA phase.

Moreover, the calculated refractive indices of both phases in PMMA/CSR/plasticizer blends are plotted in Figure 6 with the refractive index difference between the phases. It is demonstrated for the blends with TCP that the refractive indices of both phases linearly increase with the TCP content, which is attributed to the high refractive index of TCP (1.557). Similary, the refractive indices linearly decrease with the DOA content due to its low refractive index (1.445). As a result, the difference in the refractive index between PMMA and CSL core phases becomes small with increasing TCP or DOA. This is responsible for the improvement of transparency by the plasticizer addition.

Morphology of the Blends

The field-emission scanning electron microscopy images of the cryogenically fractured surface are shown in Figure 7 (PMMA/CSL)

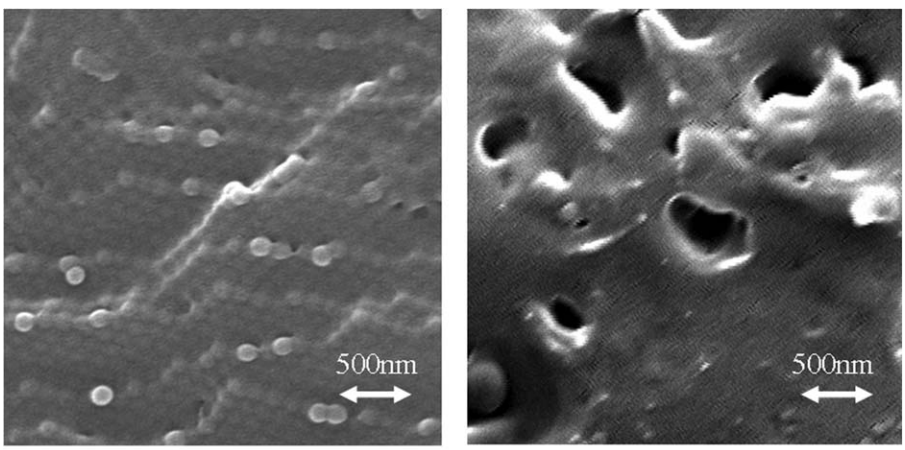

Figure 8. Field-emission scanning electron microscopy images of the ternary blends: (a) PMMA/CSL/DOA10 and (b) PMMA/CSL/DOA20.

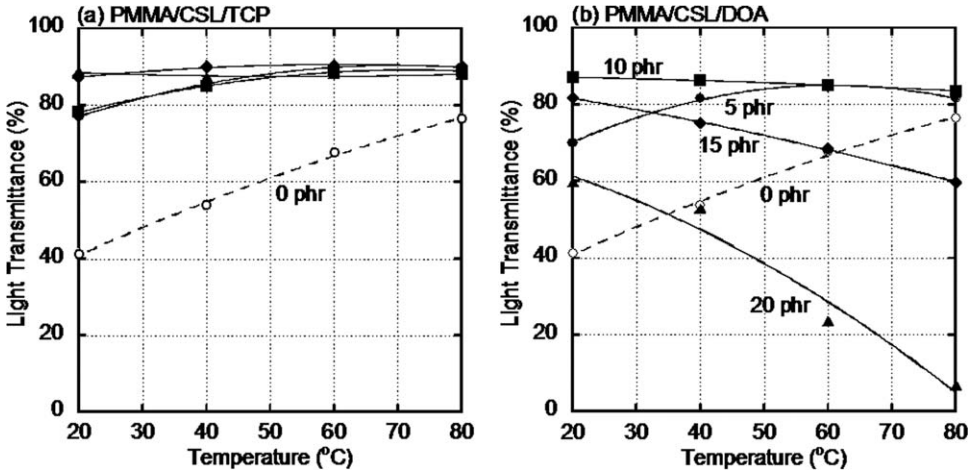

Figure 10. Temperature dependence of light transmittance for the ternary blends containing various amounts of (a) TCP and (b) DOA: 0 phr (open circles), 5 phr (closed circles), 10 phr (closed squares), 15 phr (closed diamonds), and 20 phr (closed triangles).

and Figure 8 (PMMA/CSL/plasticizer). As seen in Figure 7, phase separated morphology is clearly detected, in which spherical particles of CSL are dispersed homogeneously in a continuous phase of PMMA. The diameter is in the range of 100–200 nm, which is almost the same as that of the primary particles of CSL. Most ternary blends, except for PMMA/CSL/DOA20, also show similar morphology to that in Figure 8(a). In the case of PMMA/CSL/DOA20 [Figure 8(b)], however, the diameter of the dispersed phase is 200–500 nm, i.e., larger than that of the primary particles and comparable with the wavelength of visible light, suggesting the agglomeration of particles. This will be attributed to the poor mixing performance. Because of the large difference in the solubility parameter between PMMA and DOA, the exclusion of DOA from PMMA onto the wall of the extruder occurs, leading to slippage. This is indicated by the low torque level in the extruder, as shown in Figure 9. Consequently, particles cannot be dispersed individually because the applied shear stress is not high enough to overcome the cohesive strength of agglomerated particles, i.e., poor dispersive mixing. The large dispersed particles result in the decrease in the light transmittance by the excess light scattering as expressed by the following relation[3–6]:

$$T = \exp(-dNC_{ext}) \times 100 \quad (5)$$

where d is the film thickness, N is the number of scattering entities per unit volume, and C_{ext} is the extinction coefficient.

The extinction coefficient is given by the exact Mie theory and various approximated theories such as the simple Rayleigh scattering theory, the Rayleigh–Gans–Debye approximation, and the Anomalous Diffraction theory.[3–6] According to them, the extinction coefficient is basically determined by the refractive index difference and the diameter of particles. In other words, the key to understand the light scattering of polymer blends is the difference in the refractive index and the size of dispersed particles.[7] Apparently, the light scattering of PMMA/CSL/DOA20 is strongly affected by the size of dispersed particles, because the difference in the refractive index between two phases becomes small with increasing DOA.

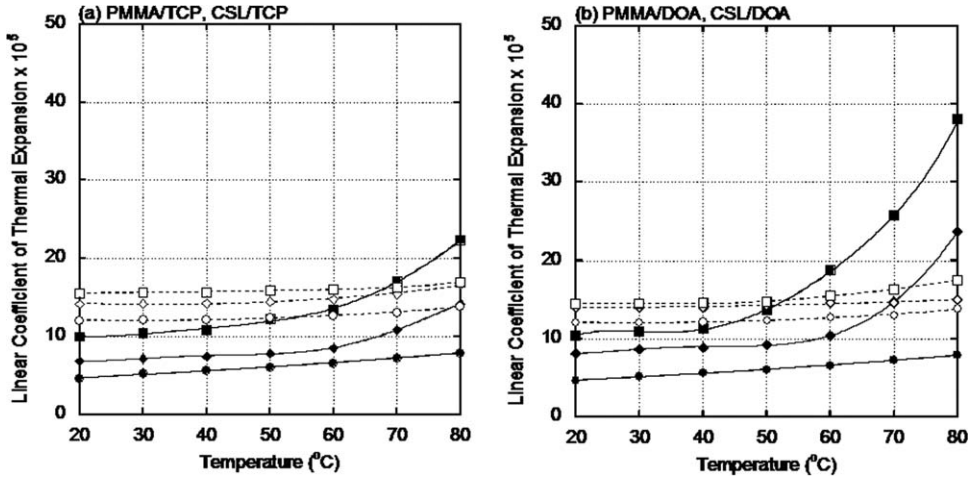

Figure 11. Linear coefficient of thermal expansion for PMMA (closed symbols) and CSL (open symbols) containing various amounts of (a) TCP and (b) DOA: 0 phr (circles), 10 phr (diamonds), and 20 phr (squares).

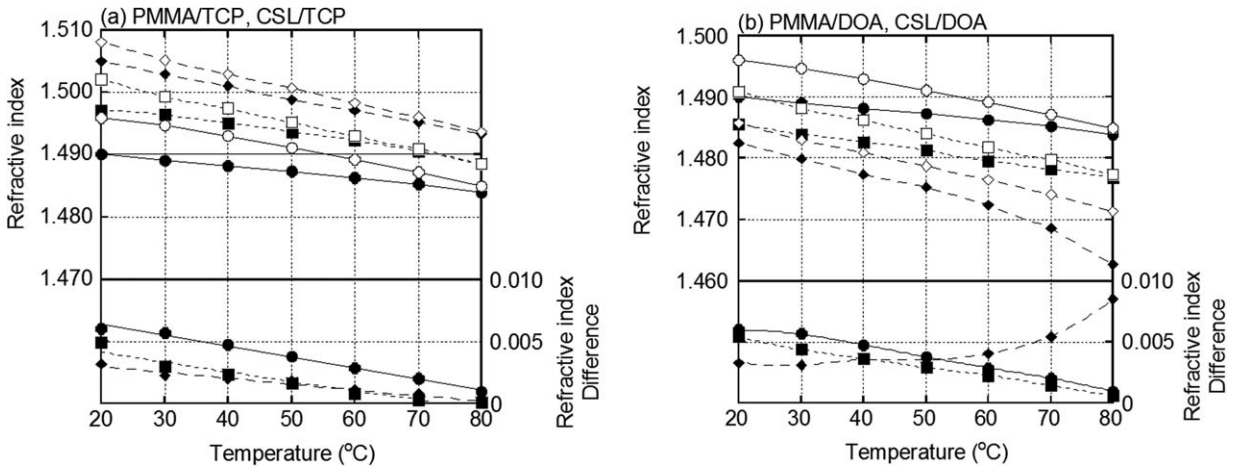

Figure 12. Refractive indices predicted by the Lorentz–Lorenz equation for PMMA (closed symbols) and CSL (open symbols) containing various amounts of (a) TCP and (b) DOA: 0 phr (circles), 10 phr (diamonds), and 20 phr (squares). The difference in the refractive index between PMMA and CSL core phases is also shown in the bottom of the figure: PMMA/CSL (closed circles), PMMA/CSL/plasticizer10 (closed diamonds), and PMMA/CSL/plasticizer20 (closed squares).

Temperature Dependence of Transparency

The temperature dependences of light transmittance for the blends containing various amounts of the plasticizers are shown in Figure 10. The transparency is significantly improved by the addition of TCP as shown in Figure 10(a). Furthermore, it should be noted that the blends containing TCP show high level of light transmittance in the wide temperature range, although the binary PMMA/CSL blend exhibits strong temperature dependence; 41% at 20°C and 77% at 80°C. On the contrary, the ternary blends containing more than 15 phr of DOA lose the transparency at high temperature as shown in Figure 10(b). The result indicates that the refractive index difference between PMMA and CSL core phases becomes large at high temperature.

The temperature dependence of the refractive index is expressed by the Lorentz–Lorenz equation.[32]

$$\frac{\partial n}{\partial T}=(n-1)\left[\frac{1}{\rho}\frac{\partial \rho}{\partial T}+\frac{1}{[R]}\frac{\partial [R]}{\partial T}\right]\cong(n-1)\frac{1}{\rho}\frac{\partial \rho}{\partial T} \quad (6)$$

$$\frac{1}{\rho}\frac{\partial \rho}{\partial T}=-3\beta \quad (7)$$

where ρ is the density, $[R]$ is the molecular refractivity, and β is the linear coefficient of thermal expansion.

As seen in the equations, the temperature dependence of the refractive index is strongly affected by the thermal expansion. In other words, information on the thermal expansion is inevitable to understand the temperature dependence of light transmittance for immiscible polymer blends. Therefore, the linear coefficient of thermal expansion for individual polymer components with and without the plasticizer was measured from 20°C to 80°C

The linear coefficient of thermal expansion for pure PMMA corresponds with the literature value (ca. 5×10^{-5}).[33] In the case of pure CSL, the value is between those for typical plastics ($4–10 \times 10^{-5}$) and rubbers ($20–25 \times 10^{-5}$),[28] which is reasonable because CSL is composed of PMMA shell and cross-linked rubber. Large thermal expansion coefficient of rubbers is attributed to the large amount of free volume, which was explained well by the WLF (Williams, Landel, and Ferry) equation.[34]

The linear expansion coefficients of PMMA and CSL increase with the plasticizer addition. In particular, the thermal expansion of plasticized PMMA is greatly enhanced at high temperature. One of the reasons is the T_g shift to lower temperatures. The broadening of relaxation time distribution also enhances the thermal expansion near T_g. However, both mechanisms cannot explain why the values are larger than those for typical rubbers. Although the detailed mechanism of the large thermal expansion of plasticized PMMA at high temperatures is unknown at present, the anharmonicity of intermolecular potential function, which is the origin of thermal expansion, seems to be enhanced by the plasticizer addition.

As compared with TCP, the DOA addition has a strong impact on the thermal expansion at high temperature despite the smaller amount in the matrix phase, as indicated in Figure 11(b). In contrast, the plasticizer addition into CSL barely increases the linear expansion coefficient.

Figure 12 shows the refractive indices of PMMA and CSL phases, calculated by the Lorentz–Lorenz equation, and the difference between them. It is well known that the refractive index of a polymer decreases with temperature. For the binary blend without plasticizers, the refractive index difference between both phases becomes small as the ambient temperature rises, because the refractive index and the linear expansion coefficient of CSL are larger than those of PMMA. Consequently, the light transmittance at 80°C is higher than that at 20°C for the binary blend, as shown in Figure 10.

The difference in the refractive index between PMMA and CSL phases in the blends with TCP is smaller than that in the blend without TCP [Figure 12(a)]. This is attributed to the increase in the temperature dependence of the refractive index, i.e., dn/dT. In fact, the slope of PMMA/TCP20 is almost the same with those of CSL and CSL/TCP blends. Consequently, the

transparency for PMMA/CSL/TCP is barely affected by the ambient temperature, as demonstrated in Figure 10(a). The effect of the DOA addition on the slope, on the other hand, is significantly strong [Figure 12(b)] as compared with the TCP addition. Therefore, only 10 phr of DOA is good enough to show the same slope with CSL and CSL/DOA blends. Furthermore, the slope of PMMA/DOA20 is steeper than those of CSL and CSL/DOA. Because the refractive index at room temperature for PMMA/DOA20 is lower than that for CSL/DOA20, the refractive index difference between PMMA/DOA20 and CSL/DOA20 increases at high temperatures. This result corresponds with the abrupt change in the temperature dependence of the transparency for PMMA/CSL blends containing more than 15 phr of DOA as shown in Figure 10(b).

CONCLUSIONS

Effect of the plasticizer addition on the transparency and its temperature dependence for the rubber-toughened blends composed of PMMA and CSL was studied using two types of plasticizers, i.e., TCP and DOA. The former one has a higher refractive index than the polymers, whereas the latter has a lower value. The addition of the plasticizer is found to enhance the transparency because it reduces the refractive index difference between PMMA and CSL core phases. Moreover, uneven distribution of the plasticizer is responsible for the excellent transparency for both systems. A large amount of DOA, however, leads to the agglomeration of CSL particles, the origin of excess light scattering, by the poor dispersive mixing due to slippage on the wall of the mixing device.

The plasticizer addition improves the transparency not only at room temperature but also in the wide temperature range. For example, the blends containing 15–20 phr of TCP or 10 phr of DOA exhibit good transparency, approximately 90% of the light transmittance, from 20°C to 80°C. On the contrary, a simple binary blend of PMMA and CSL shows the strong temperature dependence of the light transmittance owing to the difference in the temperature dependence of refractive index between a glassy PMMA and a rubbery CSL core, which is greatly affected by the difference in the thermal expansion behavior. The plasticizer addition increases the linear expansion coefficient of PMMA, whereas it barely affects the thermal expansion of CSL. As a result, the difference in the refractive index between both phases becomes small, leading to weak temperature dependence of transparency.

In this article, a new material design of a transparent rubber-toughened polymer blend is demonstrated using PMMA with CSL. Although it has been believed to be impossible for rubber-toughened blends to show good transparency in the wide temperature range, owing to the difference in the linear coefficient of thermal expansion, and thus the refractive index, this technique enables the material design. This will be used for industrial applications, including automobile parts.

REFERENCES

1. Utracki, L. A. Polymer Alloys and Blends; Carl Hanser Verlag: Munich, **1989**.
2. Roxton, T. R. *J. Appl. Polym. Sci.* **1963**, *7*, 1499.
3. Kerker, M. The Scattering of Light and Other Electromagnetic Radiation; Academic Press: San Diego, CA, **1969**.
4. Bohren, C. F.; Huffman, D. R. Absorption and Scattering of Light by Small Particles; Wiley: Weinheim, **1983**.
5. Willmouth, F. M. In Optical Properties of Polymers; Meeten, G. H., Ed.; Elsevier Applied Science: London, **1986**, Chapter 5.
6. Koike, Y.; Matuoka, S.; Bair, H. E. *Macromolecules* **1992**, *25*, 4807.
7. Khanarian G. *Polym. Eng. Sci.* **2000**, *40*, 2590.
8. Stein, R. S.; Powers, J. Topics in Polymer Physics; Imperial College Press: London, **2006**.
9. Bucknall, C. B.; Partridge, I. K.; Ward, M. V. *J. Mater. Sci.* **1984**, *19*, 2064.
10. Feng, J.; Winnik, M. A.; Shivers, R. R.; Clubb, B. *Macromolecules* **1995**, *28*, 7671.
11. Wrotecki, C.; Heim, P.; Gaillard, P. *Polym. Eng. Sci.* **1991**, *31*, 213.
12. Bucknall, C. B.; Smith, R. R. *Polymer* **1965**, *6*, 437.
13. Shah, N. *J. Mater. Sci.* **1988**, *23*, 3623.
14. Wrotecki, C.; Heim, P.; Gaillard, P. *Polym. Eng. Sci.* **1991**, *31*, 218.
15. Gloaguen, J. M.; Heim, P.; Gaillard, P.; Lefebvre, J. M. *Polymer* **1992**, *33*, 4741.
16. Lovell, P. A.; Macdonald, J.; Saunders, D. E. J.; Young, R. J. *Polymer* **1993**, *34*, 61.
17. Nelliappan, V.; Elaasser, M. S.; Klein, A.; Daniels, E. S.; Roberts, J. E.; Pearson, R. A. *J. Appl. Polym. Sci.* **1997**, *65*, 581.
18. Michler, G. H. *J. Macromol. Sci. Phys.* **1999**, *B38*, 787.
19. Baghri, R.; Pearson, R. A. *Polymer* **2000**, *41*, 269.
20. Bai, S. L.; Wang, G. T.; Hiver, J. M.; G'Sell, C. *Polymer* **2004**, *45*, 3063.
21. G'Sell, C.; Bai, S. L.; Hiver, J. M. *Polymer* **2004**, *45*, 5785.
22. Michler, G. H.; von Schmeling, H. K. *Polymer* **2013**, *54*, 3131.
23. Park, J. G.; Kim, J. Y.; Suh, K. D. *J. Appl. Polym. Sci.* **1998**, *69*, 2291.
24. Song, J. Y.; Kim, J. W.; Suh, K. D. *J. Appl. Polym. Sci.* **1999**, *71*, 1607.
25. Bernini, U.; Carbonara, G.; Malinconico, M.; Mormile, P.; Russo, P.; Volpe, M. G. *Appl. Opt.* **1992**, *31*, 5794.
26. Bernini, U.; Malinconico, M.; Matruscelli, E.; Mormile, P.; Novellino, A.; Russo, P.; Volpe, M. G. *J. Mater. Process. Technol.* **1995**, *55*, 224.
27. Errico, M. E.; Greco, R.; Laurienzo, P.; Malinconico, M.; Viscardo, D. *J. Appl. Polym. Sci.* **2006**, *99*, 2926.
28. van Krevelen, D. W.; te Nijenhuis, K. Properties of Polymers, 4th ed.; Elsevier: Amsterdam, **2009**, Chapter 4, pp 89.
29. Seferis, J. C.; Samnels, R. J. *Polym. Eng. Sci.* **1979**, *19*, 975.
30. Wedgewood, A. R.; Seferis, J. C. *Polym. Eng. Sci.* **1984**, *24*, 328.

31. Brandrup, J.; Immergut, E. H. Polymer Handbook, 3rd ed.; Wiley-Interscience: New York, **1989**.
32. Choi, J. H.; Eichele, C.; Lin, Y. C.; Shi, F. G.; Carlson, R.; Sciamanna, S. *Scripta Materialia* **2008**, *58*, 413.
33. Riha, P.; Hadac, J.; Slobodian, P.; Saha, P.; Rychwalski, R. W.; Kubat, J. *Polymer* **2007**, *48*, 7356.
34. Ferry, J. D. Viscoelastic Properties of Polymers, 3rd ed.; Wiley: New York, **1980**.